Electronic Supplementary Information

3D lanthanide-coordination frameworks constructed by a ternary mixed-ligand: crystal structure, luminescence and luminescence sensing

Qi-Wei Xu, Gaoyun Dong, Ruifang Cui and Xia Li*

Department of Chemistry, Capital Normal University, Beijing, 100048, China.

Table of Contents

1. The PXRD patterns of Ln-MOF. (Fig. S1)

2. N_2 sorption isotherm at 77 K under 1 bar of Eu-MOF. (Fig. S2)

3. TG curve of Eu-MOF. (Fig. S3)

4. PXRD patterns of Eu-MOF in different organic solvents and in aqueous solution with different pH for 3 days. (Fig. S4)

5. The solid state emission spectra of Gd-MOF and the ligands. (Fig. S5)

6. CIE image of Ln-MOFs. (Fig. S6)

7. Emission patterns of Eu-MOF in different excitation wavelengths. (Fig. S7)

8. CIE image (1, H_2O; 2, ethyl acetate; 3, THF; 4, acetone; 5, CH_3CN; 6, CH_3OH; 7, EtOH; 8, CH_2Cl_2; 9, isopropanol; 10, DMF). (Fig. S8)

9. The chemical structures of quercetin, catechin, daidzein, catechol, resorcin and hydroquinone. (Fig. S9)

10. PXRD patterns of Eu-MOF after luminescence sensing for quercetin and Fe^{3+}.(Fig. S10)

11. UV–Vis absorption spectra of other analogues with excitation spectrum of Eu-MOF (372 nm, the maximum absorption of quercetin). (Fig. S11)

12. The luminescence intensity of Eu-MOF in different cations with and without the Fe^{3+}. (Fig. S12)

13. The UV–Vis absorption spectra of metal ions and Eu-MOF. (Fig. S13)

14. (a) Emission spectra of Eu-MOF dispersed in ethanol solution containing different metal ions, (b) Emission intensity of Eu-MOF at 616 nm ($^5D_0 \rightarrow {}^7F_2$), (c) Emission spectra of Eu-MOF with the addition of the Fe^{3+}, (d) the Stern−Volmer plot for the quenching of Eu-MOF in ethanol solution. (Fig. S14)

15. (a) Emission spectra of Eu-MOF dispersed in acetone solution containing different metal ions, (b) Emission intensity of Eu-MOF at 616 nm ($^5D_0 \rightarrow {}^7F_2$), (c) Emission spectra of Eu-MOF with the addition of the Fe^{3+},(d) the Stern−Volmer plot for the quenching of Eu-MOF in acetone solution. (Fig. S15)

16. (a) Emission spectra of Eu-MOF dispersed in acetonitrile solution containing different metal ions, (b) Emission intensity of Eu-MOF at 616 nm ($^5D_0 \rightarrow {}^7F_2$), (c) Emission spectra of Eu-MOF with the addition of the Fe^{3+}, (d) the Stern−Volmer plot for the quenching of Eu-MOF in acetonitrile solution. (Fig. S16)

17. (a) Emission spectra of Eu-MOF dispersed in ethyl acetate solution containing different metal ions, (b) Emission intensity of Eu-MOF at 616 nm ($^5D_0 \rightarrow {}^7F_2$), (c) Emission spectra of Eu-MOF with the addition of the Fe^{3+}, (d) the Stern−Volmer plot for the quenching of Eu-MOF in ethyl acetate solution. (Fig. S17)

18. Selected bond lengths [Å] and angles [°] for complexes **1-5**. (Table S1)

19. A Comparison of the Detection Limits of Fe^{3+} with Other Reported. (Table S2)

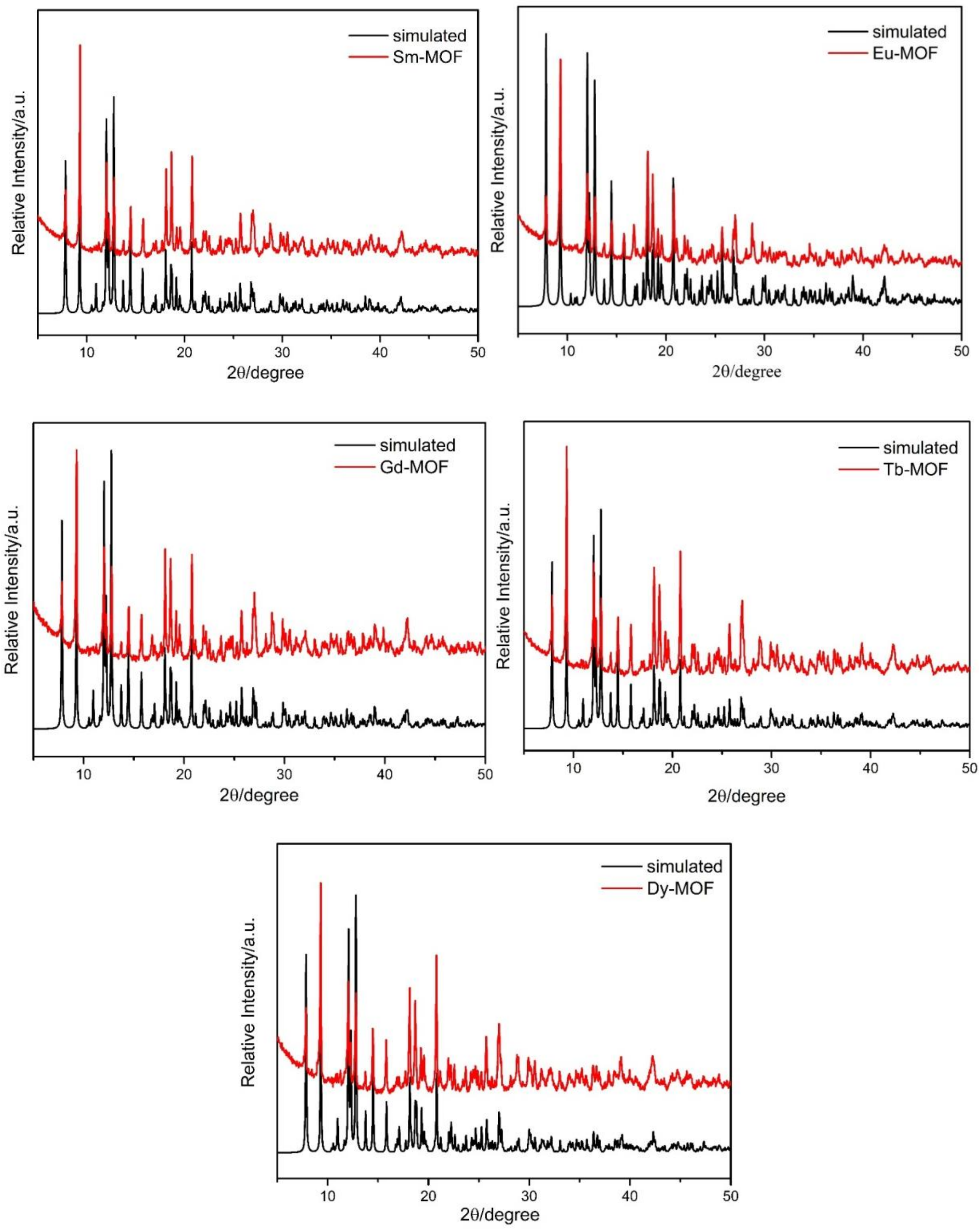

Fig. S1 The PXRD patterns of Ln-MOFs.

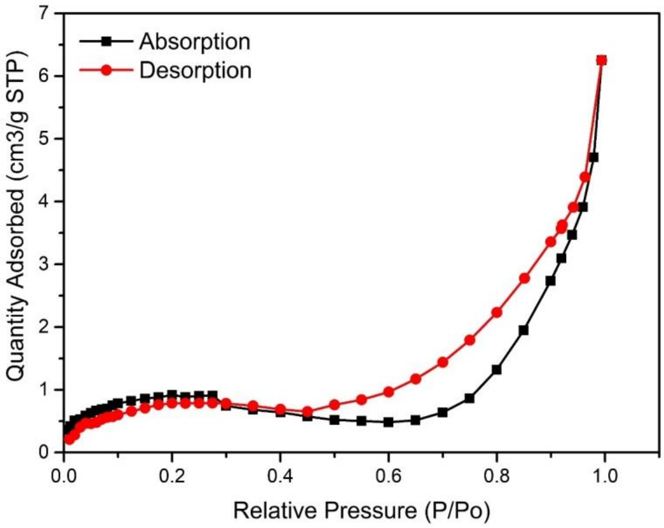

Fig. S2 N_2 sorption isotherm at 77 K under 1 bar of Eu-MOF.

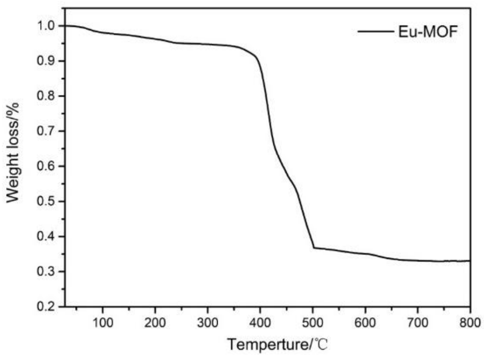

Fig. S3 TG curve of Eu-MOF.

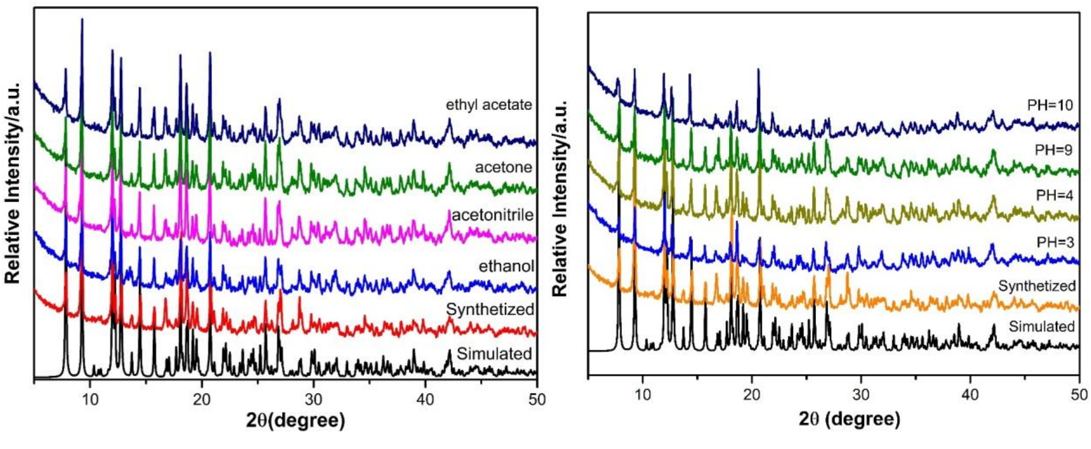

Fig. S4 PXRD patterns of Eu-MOF in different organic solvents and in aqueous solution with different pH for 3 days.(The Eu-MOF samples were dispersed in different organic solvents or in aqueous solution (pH = 3, 4, 9, 10), and then were sonicated (10 min). After 3 days, the ground solid samples were collected, washed with deionized water and desiccated for PXRD testing.)

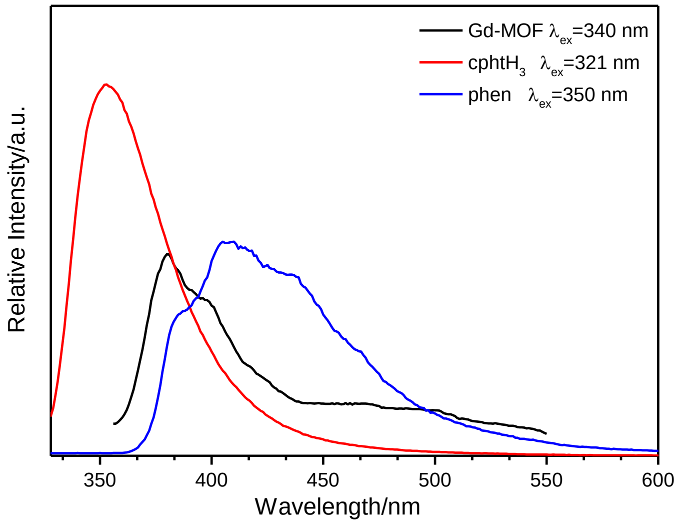

Fig. S5 The solid state emission spectra of Gd-MOF and the ligands.

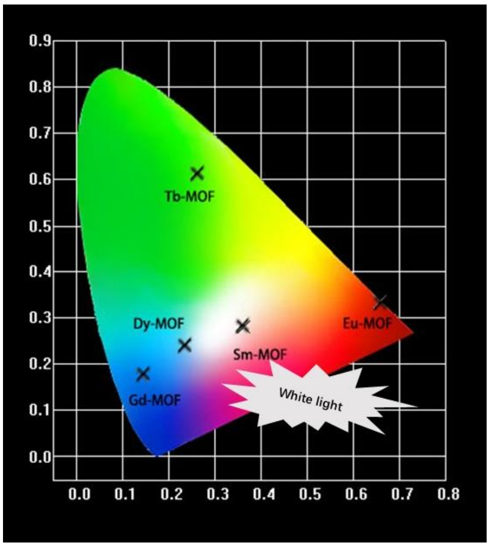

Fig. S6 CIE image of Ln-MOFs.

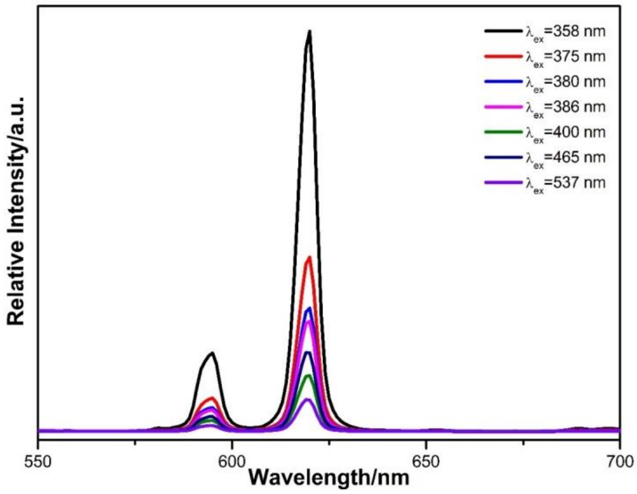

Fig. S7 Emission patterns of Eu-MOF in different excitation wavelengths.

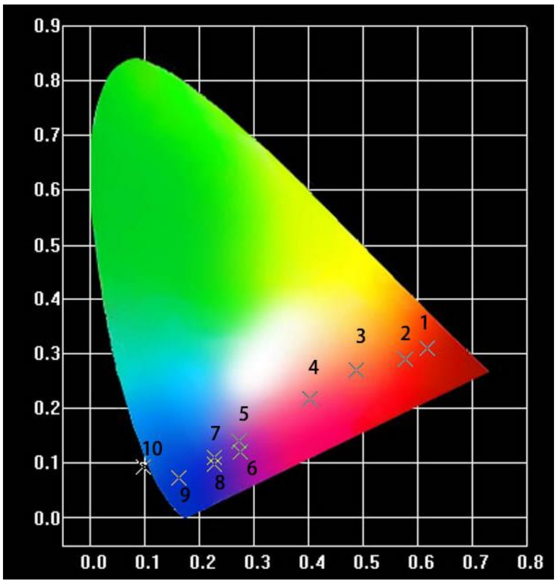

Fig. S8 CIE image(1, H_2O; 2, ethyl acetate; 3, THF; 4, acetone; 5, CH_3CN; 6, CH_3OH; 7, EtOH; 8, CH_2Cl_2; 9, isopropanol; 10, DMF).

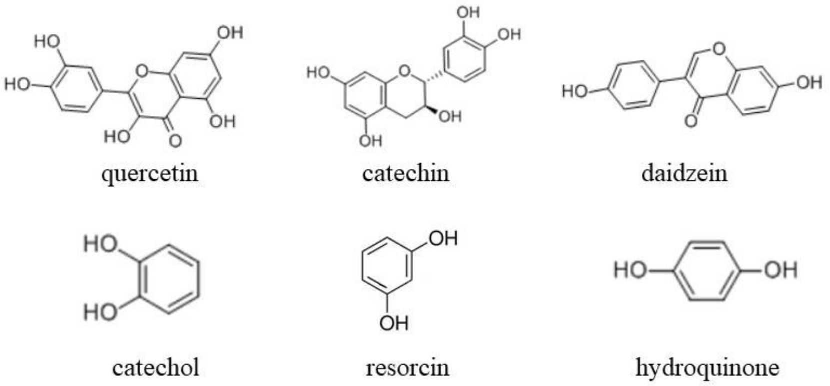

Fig. S9 The chemical structures of quercetin, catechin, daidzein, catechol, resorcin and hydroquinone.

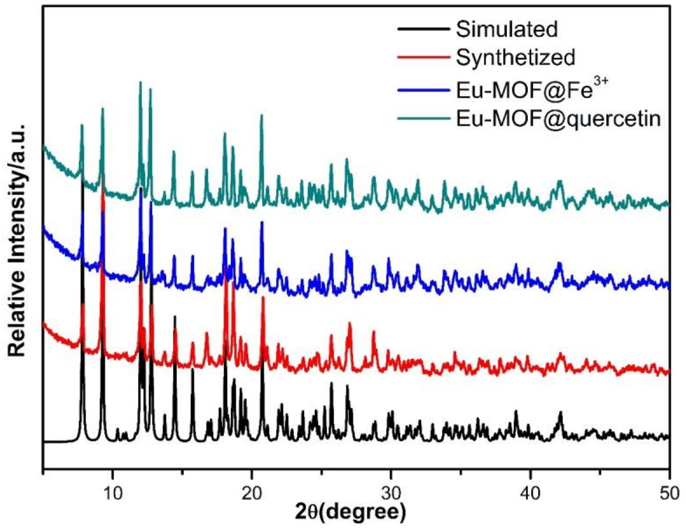

Fig. S10 PXRD patterns of Eu-MOF after luminescence sensing for quercetin and Fe^{3+}.

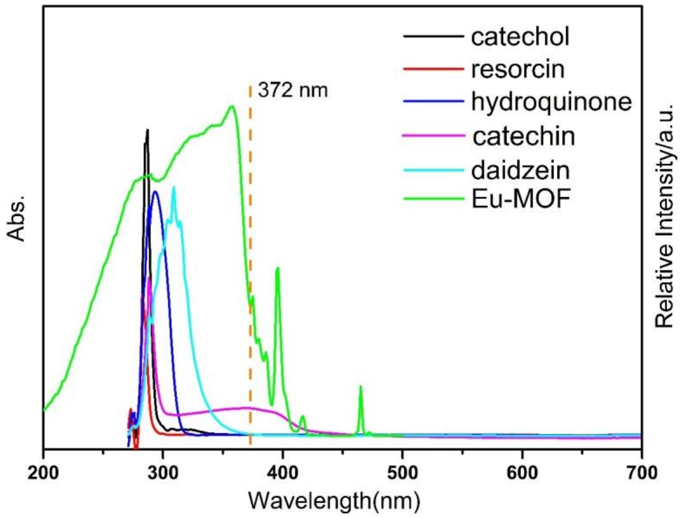

Fig. S11 UV–Vis absorption spectra of other analogues with excitation spectrum of Eu-MOF (372 nm, the maximum absorption of quercetin).

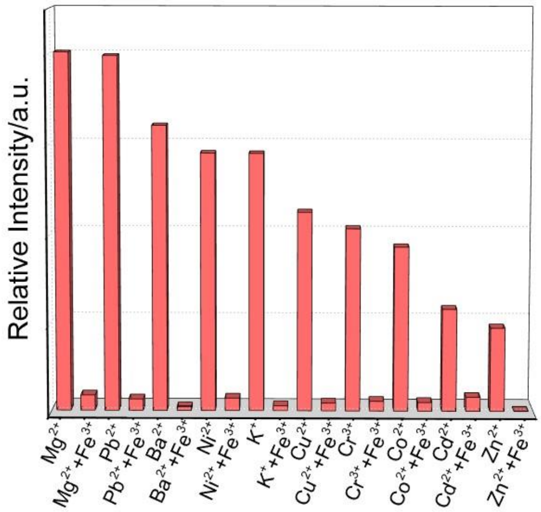

Fig. S12 The luminescence intensity of Eu-MOF in different cations with and without the Fe^{3+}.

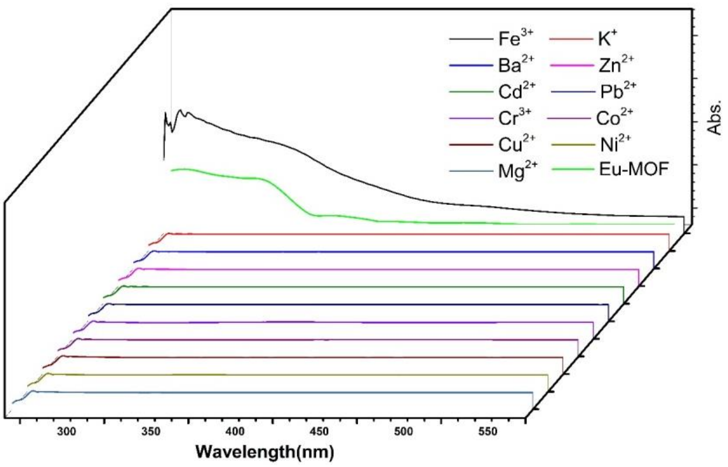

Fig. S13 The UV–Vis absorption spectra of metal ions and Eu-MOF.

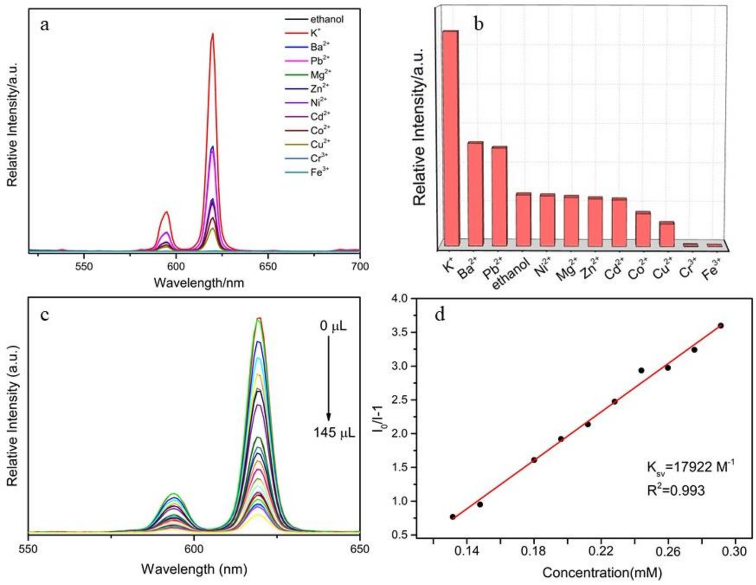

Fig. S14 (a) Emission spectra of Eu-MOF dispersed in ethanol solution containing different metal ions, (b) Emission intensity of Eu-MOF at 616 nm ($^5D_0 \rightarrow {}^7F_2$), (c) Emission spectra of Eu-MOF with the addition of the Fe^{3+}, (d) the Stern−Volmer plot for the quenching of Eu-MOF in ethanol solution.

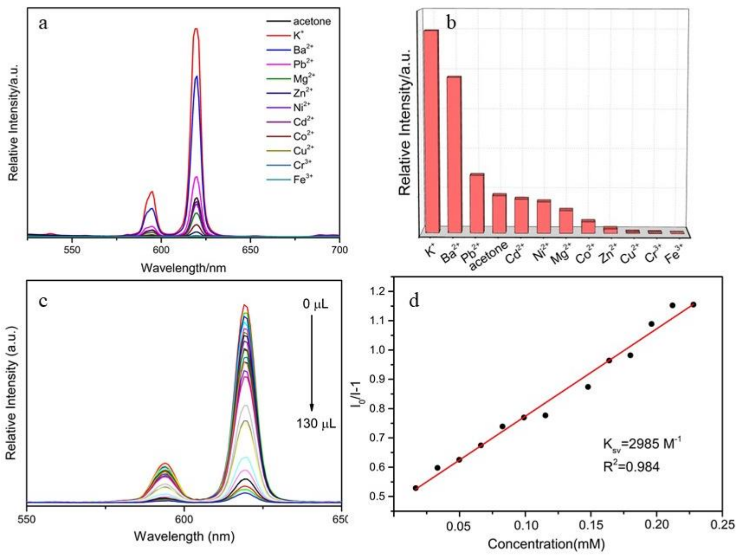

Fig. S15 (a) Emission spectra of Eu-MOF dispersed in acetone solution containing different metal ions, (b) Emission intensity of Eu-MOF at 616 nm ($^5D_0 \rightarrow {}^7F_2$),(c) Emission spectra of Eu-MOF with the addition of the Fe^{3+},(d) the Stern−Volmer plot for the quenching of Eu-MOF in acetone solution.

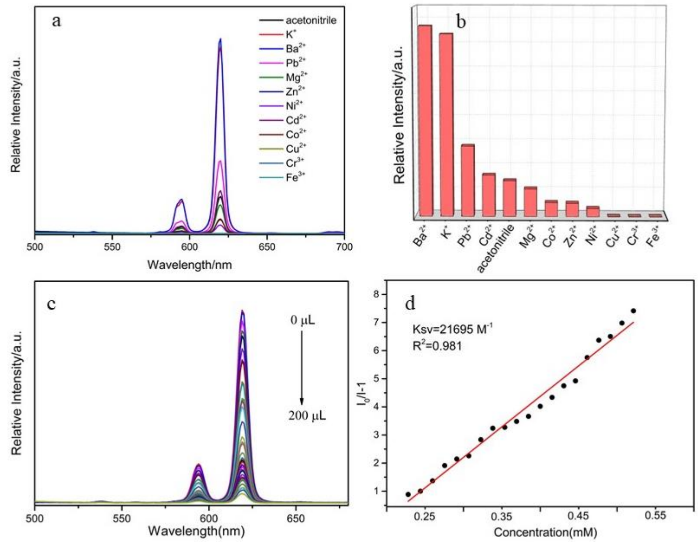

Fig. S16 (a) Emission spectra of Eu-MOF dispersed in acetonitrile solution containing different metal ions, (b) Emission intensity of Eu-MOF at 616 nm ($^5D_0\rightarrow{}^7F_2$), (c) Emission spectra of Eu-MOF with the addition of the Fe^{3+}, (d) the Stern−Volmer plot for the quenching of Eu-MOF in acetonitrile solution.

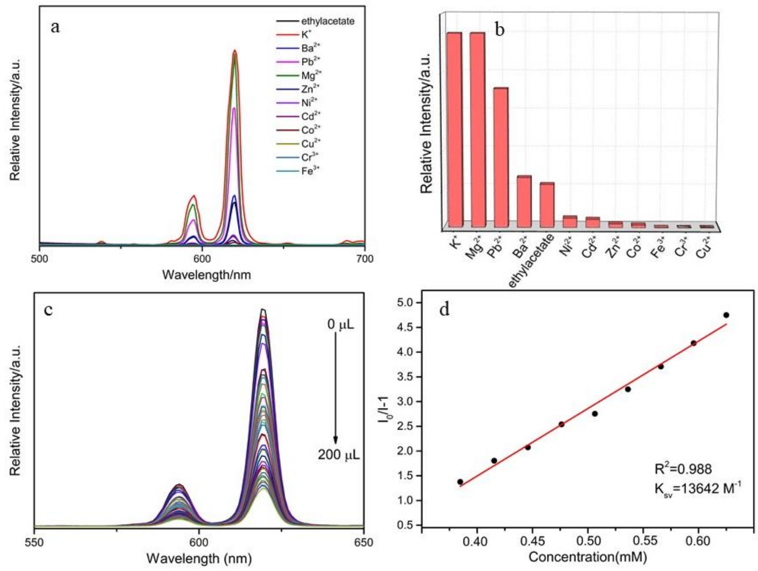

Fig. S17 (a) Emission spectra of Eu-MOF dispersed in ethyl acetate solution containing different metal ions, (b) Emission intensity of Eu-MOF at 616 nm ($^5D_0\rightarrow{}^7F_2$), (c) Emission spectra of Eu-MOF with the addition of the Fe^{3+}, (d) the Stern−Volmer plot for the quenching of Eu-MOF in ethyl acetate solution.

Table S1 Selected bond lengths [Å] and angles [°] for complexes **1-5**.

		1	
Sm(1)-O(5)A	2.388(3)	Sm(1)-O(8)	2.406(4)
Sm(1)-O(3)	2.437(3)	Sm(1)-O(4)B	2.472(3)
Sm(1)-O(7)C	2.481(3)	Sm(1)-O(6)C	2.488(3)
Sm(1)-O(1)B	2.497(3)	Sm(1)-N(2)	2.599(4)
Sm(1)-N(1)	2.623(4)		
O(5)A-Sm(1)-O(8)	81.34(11)	O(5)A-Sm(1)-O(3)	67.85(10)
O(8)-Sm(1)-O(3)	133.11(11)	O(5)A-Sm(1)-O(4)B	131.62(11)
O(8)-Sm(1)-O(4)B	76.19(11)	O(3)-Sm(1)-O(4)B	98.32(11)
O(5)A-Sm(1)-O(7)C	75.43(11)	O(8)-Sm(1)-O(7)C	71.44(11)
O(3)-Sm(1)-O(7)C	128.46(11)	O(4)B-Sm(1)-O(7)C	133.22(11)
O(5)A-Sm(1)-O(6)C	128.55(11)	O(8)-Sm(1)-O(6)C	79.92(11)
O(3)-Sm(1)-O(6)C	146.97(11)	O(4)B-Sm(1)-O(6)C	88.86(11)
O(7)C-Sm(1)-O(6)C	53.21(11)	O(5)A-Sm(1)-O(1)B	79.91(11)
O(8)-Sm(1)-O(1)B	72.39(11)	O(3)-Sm(1)-O(1)B	68.18(10)
O(4)B-Sm(1)-O(1)B	52.65(11)	O(7)C-Sm(1)-O(1)B	138.62(11)
O(6)C-Sm(1)-O(1)B	136.51(11)	O(5)A-Sm(1)-N(2)	83.52(12)
O(8)-Sm(1)-N(2)	140.56(12)	O(3)-Sm(1)-N(2)	71.47(11)
O(4)B-Sm(1)-N(2)	137.85(13)	O(7)C-Sm(1)-N(2)	69.56(12)
O(6)C-Sm(1)-N(2)	81.59(11)	O(1)B-Sm(1)-N(2)	139.61(11)
O(5)A-Sm(1)-N(1)	134.60(12)	O(8)-Sm(1)-N(1)	143.85(13)
O(3)-Sm(1)-N(1)	72.72(11)	O(4)B-Sm(1)-N(1)	74.92(12)
O(7)C-Sm(1)-N(1)	115.43(12)	O(6)C-Sm(1)-N(1)	78.24(12)
O(1)B-Sm(1)-N(1)	105.59(12)	N(2)-Sm(1)-N(1)	62.96(14)
		2	
Eu(1)-O(8)	2.371(3)	Eu(1)-O(1)A	2.398(3)
Eu(1)-O(9)	2.443(3)	Eu(1)-O(4)B	2.458(3)
Eu(1)-O(6)	2.468(3)	Eu(1)-O(7)	2.483(3)
Eu(1)-O(5)B	2.497(3)	Eu(1)-N(2)	2.590(4)
Eu(1)-N(1)	2.619(4)		
O(8)-Eu(1)-O(1)A	81.28(12)	O(8)-Eu(1)-O(9)	67.88(9)
O(1)A-Eu(1)-O(9)	133.40(11)	O(8)-Eu(1)-O(4)B	131.53(10)
O(1)A-Eu(1)-O(4)B	75.92(11)	O(9)-Eu(1)-O(4)B	98.84(10)
O(8)-Eu(1)-O(6)	75.75(10)	O(1)A-Eu(1)-O(6)	71.46(12)
O(9)-Eu(1)-O(6)	128.42(11)	O(4)B-Eu(1)-O(6)	132.74(11)
O(8)-Eu(1)-O(7)	128.57(10)	O(1)A-Eu(1)-O(7)	79.65(12)
O(9)-Eu(1)-O(7)	146.94(11)	O(4)B-Eu(1)-O(7)	88.55(11)
O(6)-Eu(1)-O(7)	52.93(11)	O(8)-Eu(1)-O(5)B	79.90(10)
O(1)A-Eu(1)-O(5)B	72.43(12)	O(9)-Eu(1)-O(5)B	68.52(10)
O(4)B-Eu(1)-O(5)B	52.66(10)	O(6)-Eu(1)-O(5)B	138.84(11)
O(7)-Eu(1)-O(5)B	136.25(11)	O(8)-Eu(1)-N(2)	83.70(11)

O(1)A-Eu(1)-N(2)	140.47(12)	O(9)-Eu(1)-N(2)	71.28(11)
O(4)B-Eu(1)-N(2)	138.04(11)	O(6)-Eu(1)-N(2)	69.46(12)
O(7)-Eu(1)-N(2)	81.69(12)	O(5)B-Eu(1)-N(2)	139.77(12)
O(8)-Eu(1)-N(1)	134.71(11)	O(1)A-Eu(1)-N(1)	143.76(13)
O(9)-Eu(1)-N(1)	72.50(10)	O(4)B-Eu(1)-N(1)	74.93(11)
O(6)-Eu(1)-N(1)	115.46(11)	O(7)-Eu(1)-N(1)	78.56(12)
O(5)B-Eu(1)-N(1)	105.30(12)	N(2)-Eu(1)-N(1)	63.15(12)
		3	
Gd(1)-O(9)A	2.359(2)	Gd(1)-O(1)	2.381(3)
Gd(1)-O(8)	2.432(2)	Gd(1)-O(4)B	2.445(2)
Gd(1)-O(7)C	2.463(3)	Gd(1)-O(6)C	2.476(3)
Gd(1)-O(5)B	2.493(3)	Gd(1)-N(18)	2.576(3)
Gd(1)-N(1)	2.609(3)		
O(9)A-Gd(1)-O(1)	80.78(10)	O(9)A-Gd(1)-O(8)	68.11(8)
O(1)-Gd(1)-O(8)	133.29(10)	O(9)A-Gd(1)-O(4)B	131.58(9)
O(1)-Gd(1)-O(4)B	75.79(10)	O(8)-Gd(1)-O(4)B	99.31(9)
O(9)A-Gd(1)-O(7)C	75.69(9)	O(1)-Gd(1)-O(7)C	71.35(10)
O(8)-Gd(1)-O(7)C	128.45(9)	O(4)B-Gd(1)-O(7)C	132.24(9)
O(9)A-Gd(1)-O(6)C	128.76(9)	O(1)-Gd(1)-O(6)C	79.83(11)
O(8)-Gd(1)-O(6)C	146.89(10)	O(4)B-Gd(1)-O(6)C	87.89(9)
O(7)C-Gd(1)-O(6)C	53.20(9)	O(9)A-Gd(1)-O(5)B	79.92(9)
O(1)-Gd(1)-O(5)B	72.82(11)	O(8)-Gd(1)-O(5)B	68.21(9)
O(4)B-Gd(1)-O(5)B	52.92(9)	O(7)C-Gd(1)-O(5)B	139.18(10)
O(6)C-Gd(1)-O(5)B	136.24(10)	O(9)A-Gd(1)-N(18)	83.86(10)
O(1)-Gd(1)-N(18)	140.34(11)	O(8)-Gd(1)-N(18)	71.25(10)
O(4)B-Gd(1)-N(18)	138.23(10)	O(7)C-Gd(1)-N(18)	69.48(10)
O(6)C-Gd(1)-N(18)	81.86(11)	O(5)B-Gd(1)-N(18)	139.43(10)
O(9)A-Gd(1)-N(1)	135.05(9)	O(1)-Gd(1)-N(1)	143.90(11)
O(8)-Gd(1)-N(1)	72.49(9)	O(4)B-Gd(1)-N(1)	74.95(10)
O(7)C-Gd(1)-N(1)	115.60(10)	O(6)C-Gd(1)-N(1)	78.43(10)
O(5)B-Gd(1)-N(1)	104.83(10)	N(18)-Gd(1)-N(1)	63.35(10)
		4	
Tb(1)-O(8)A	2.349(4)	Tb(1)-O(1)	2.375(4)
Tb(1)-O(9)	2.423(4)	Tb(1)-O(4)B	2.435(4)
Tb(1)-O(7)C	2.449(4)	Tb(1)-O(6)C	2.459(4)
Tb(1)-O(5)B	2.471(4)	Tb(1)-N(2)	2.559(5)
Tb(1)-N(1)	2.593(5)		
O(8)A-Tb(1)-O(1)	80.83(15)	O(8)A-Tb(1)-O(9)	68.30(12)
O(1)-Tb(1) -O(9)	133.08(14)	O(8)A-Tb(1)-O(4)B	131.81(12)
O(1)-Tb(1) -O(4)B	75.59(14)	O(9)-Tb(1) -O(4)B	99.22(13)
O(8)A-Tb(1)-O(7)C	75.29(13)	O(1)-Tb(1)-O(7)C	71.40(14)
O(9)-Tb(1) -O(7)C	128.58(14)	O(4)B-Tb(1)-O(7)C	132.20(13)

O(8)A-Tb(1)-O(6)C	129.08(13)	O(1)-Tb(1) -O(6)C	79.95(16)
O(9)-Tb(1)-O(6)C	146.96(14)	O(4)B-Tb(1)-O(6)C	87.28(14)
O(7)C-Tb(1)-O(6)C	53.92(13)	O(8)A-Tb(1)-O(5)B	79.99(13)
O(1)-Tb(1) -O(5)B	72.72(15)	O(9)-Tb(1)-O(5)B	67.90(13)
O(4)B-Tb(1)-O(5)B	53.12(13)	O(7)C-Tb(1)-O(5)B	138.97(14)
O(6)C-Tb(1)-O(5)B	135.98(14)	O(8)A-Tb(1)-N(2)	83.58(14)
O(1)-Tb(1) -N(2)	140.35(15)	O(9)-Tb(1) -N(2)	71.49(14)
O(4)B-Tb(1)-N(2)	138.43(14)	O(7)C-Tb(1)-N(2)	69.44(15)
O(6)C-Tb(1)-N(2)	82.16(15)	O(5)B-Tb(1)-N(2)	139.35(15)
O(8)A-Tb(1)-N(1)	135.12(14)	O(1)-Tb(1) -N(1)	143.74(16)
O(9)-Tb(1) -N(1)	72.40(14)	O(4)B-Tb(1)-N(1)	74.72(14)
O(7)C-Tb(1)-N(1)	116.10(15)	O(6)C-Tb(1)-N(1)	78.31(15)
O(5)B-Tb(1)-N(1)	104.56(15)	N(2)-Tb(1)-N(1)	63.79(15)
		5	
Dy(1)-O(8)	2.335(3)	Dy(1)-O(1)A	2.357(3)
Dy(1)-O(9)B	2.412(3)	Dy(1)-O(6)	2.419(3)
Dy(1)-O(5)C	2.443(3)	Dy(1)-O(4)C	2.436(3)
Dy(1)-O(7)	2.466(3)	Dy(1)-N(2)	2.550(4)
Dy(1)-N(1)	2.588(4)		
O(8)-Dy(1)-O(1)A	80.52(12)	O(8)-Dy(1)-O(9)B	68.78(10)
O(1)A-Dy(1)-O(9)B	133.37(12)	O(8)-Dy(1)-O(6)	131.83(10)
O(1)A-Dy(1)-O(6)	75.63(12)	O(9)B-Dy(1)-O(6)	99.30(10)
O(8)-Dy(1)-O(5)C	129.07(11)	O(1)A-Dy(1)-O(5)C	79.96(13)
O(9)B-Dy(1)-O(5)C	146.65(11)	O(6)-Dy(1)-O(5)C	87.02(11)
O(8)-Dy(1)-O(4)C	75.54(10)	O(1)A-Dy(1)-O(4)C	71.24(12)
O(9)B-Dy(1)-O(4)C	128.96(11)	O(6)-Dy(1)-O(4)C	131.74(11)
O(5)C-Dy(1)-O(4)C	53.68(11)	O(8)-Dy(1)-O(7)	79.73(10)
O(1)A-Dy(1)-O(7)	72.62(12)	O(9)B-Dy(1)-O(7)	68.12(11)
O(6)-Dy(1)-O(7)	53.45(10)	O(5)C-Dy(1)-O(7)	135.98(12)
O(4)C-Dy(1)-O(7)	138.84(12)	O(8)-Dy(1)-N(2)	83.50(11)
O(1)A-Dy(1)-N(2)	140.09(12)	O(9)B-Dy(1)-N(2)	71.31(11)
O(6)-Dy(1)-N(2)	138.68(11)	O(5)C-Dy(1)-N(2)	82.33(12)
O(4)C-Dy(1)-N(2)	69.43(12)	O(7)-Dy(1)-N(2)	139.34(12)
O(8)-Dy(1)-N(1)	135.45(11)	O(1)A-Dy(1)-N(1)	143.75(13)
O(9)B-Dy(1)-N(1)	72.20(11)	O(6)-Dy(1)-N(1)	74.72(11)
O(5)C-Dy(1)-N(1)	78.13(12)	O(4)C-Dy(1)-N(1)	115.85(12)
O(7)-Dy(1)-N(1)	104.89(12)	N(2)-Dy(1)-N(1)	64.04(12)

Symmetry transformations used to generate equivalent atoms:

For **1**: A: 1-X,-Y,-Z; B: -X,-1/2+Y,-1/2-Z; C: -X,-Y,-1-Z

For **2**: A: 1-X,-1-Y,-Z; B: +X,-1/2-Y,-1/2+Z; C: -X,-1-Y,-1-Z

For **3**: A: -X,-1-Y,-Z; B: -1-X,1/2+Y,-1/2-Z; C: -1-X,-1-Y,-1-Z

For **4**: A: 1-X,-Y,-Z; B: -X,-1/2+Y,-1/2-Z; C: -X,-Y,-1-Z

For **5**: A: -1-X,-1/2+Y,-1/2-Z; B: -X,-1-Y,-Z; C: +X,-1/2-Y,-1/2+Z

Table S2 A Comparison of the Detection Limits of Fe^{3+} with Other Reported

	Method used	Solvent	LOD	Reference
Eu-MOF	LD	acetone	0.473 mM	This work
Eu-MOF	LD	acetonitrile	0.065 mM	This work
Eu-MOF	LD	Ethyl acetate	0.103 mM	This work
Eu-MOF	LD	water	0.336 mM	This work
Eu-MOF	LD	water	0.023 mM	S1
Zn-MOF	LD	water	0.220 mM	S2
Co-MOF	LD	methanol	0.616 mM	S4
Co-MOF	LD	ethanol	0.264mM	S4
Eu-MOF	LD	ethanol	0.026 mM	S3
Eu-MOF	LD	ethanol	0.078 mM	This work
Tb-MOF	LD	DMF	10^{-3} mM	S5

LD = luminescent detection

References

S1. Y. L. Gai, Q. Guo, X. Y. Zhao, Y. Chen, S. Liu, Y. Zhang, C. X. Zhuo, C. Yao and K. C. Xiong, *Dalton Trans.*, 2018, **47**, 12051-12055.

S2. W.-Q. Tong, W.-N. Liu, L.-L. Ma, Y. Wang, J.-M. Wang, L. Hou, Y.-Y. Wang, *Dalton Trans.*. 2019, **48**, 7786-7793.

S3. G. P. Li, G. Liu, Y. Z. Li, L. Hou, Y. Y. Wang and Z. Zhu, *Inorg. Chem.*, 2016, **55**, 3952.

S4. Y. Li, X. Wang, C. Xing, X. Zhang, Z. Liang, X. Wang, K. Zhang, Y. Wang, D. Liu, W. Fan and F. Dai, *Chinese Chemical Letters*, 2019, **30**, 1440-1444.

S5. Q. Zhang, J. Wang, A. M. Kirillov, W. Dou, C. Xu, C. Xu, L. Yang, R. Fang and W. Liu, *ACS Appl. Mater. Interfaces*, 2018, **10**, 23976-23986.